THE JOURNAL OF PHYSICAL CHEMISTRY C
A JOURNAL OF THE AMERICAN CHEMICAL SOCIETY

pubs.acs.org/JPCC
Article

Ca Mobility in NASICON Battery Materials Studied from First-Principles

Published as a part of The Journal of Physical Chemistry C special issue "Francesc Illas and Gianfranco Pacchioni Festschrift".

Katharina Helmbrecht* and Axel Groß

Cite This: https://doi.org/10.1021/acs.jpcc.4c08058

ABSTRACT: Batteries using multivalent charge carriers present a promising alternative to traditional Li-ion technology, offering the potential for higher energy densities and often relying on more abundant elements. However, their ion mobility within the electrolyte and cathode is generally lower than that of monovalent carriers due to stronger electrostatic interactions, heightening the need for materials that can provide high ion mobility. NASICON materials are known for their high ion mobility with monovalent carriers such as lithium and sodium and are widely used as solid electrolytes. In this computational study, we investigate two NASICON materials in particular with respect to their ion mobility for the bivalent charge carrier calcium, focusing on how the transition metal's atomic size in the NASICON material influences the height of the migration barrier and the properties of the materials as a solid electrolyte or electrode material. We found both materials to be good candidates for solid electrolytes with sufficiently low ion migration barriers. We confirm that the triangular faces of the octahedra along the reaction path whose size scales with the radii of the transition metal atoms act as the bottlenecks for migration.

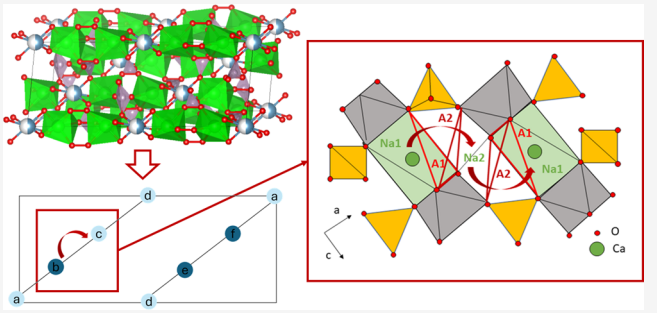

INTRODUCTION

Today, most of the demand for portable energy storage is met by lithium−ion batteries (LIBs), which is largely due to their extraordinary performance, including high energy density, operating voltage, and long life cycle.[1,2] However, problems arise in sourcing the needed lithium and cobalt metal,[3] meaning that state-of-the-art LIBs may not be able to fulfill the growing demand for energy storage solutions. Hence, alternative battery concepts and new battery materials are needed, which allow for sustainable, safe, compact, and high-voltage energy storage systems.[4−6] While it seems unlikely that alternative battery technologies will be able to surpass Li in the area of portable batteries, there is also a growing demand for stationary energy storage and heavy-duty systems. The requirements of those can, on the other hand, be met by a variety of battery types.

NASICON sodium (Na) superionic conductor structures exhibit great structural stability and high ionic conductivity—especially for sodium ions.[7] They belong to the family of superionic conductors, which are materials that display exceptionally high ionic conductivity at or near room temperature.[8] Furthermore, they are classified as polyanionic compounds, meaning they contain anions with multiple negative charges, such as the characteristic tetrahedral anionic units XO_4, or their derivatives.[9] The NASICON structure contains two distinct positions for monovalent ions, usually called Na1 and Na2 sites. In contrast, multivalent ions like magnesium or calcium typically only occupy the Na1-position within the NASICON framework because of their higher charge. This leads to a lower occupation of crystal sites[10] with the Na2 site becoming energetically much more unfavorable for bivalent ions, except for some sulfur structures in which Na2 positions can also be occupied as they are also energetically favorable.[11] The missing occupation of the Na2 sites leads to a higher structural rigidity of the crystal structure, which reduces structural changes upon intercalation/deintercalation. Furthermore, this also leads to a different energetic shape of the diffusion path, as there is no intermediate stable state at Na2, and to a less facile migration caused by the increased electrostatic interactions with the framework.[10]

Received: November 29, 2024
Revised: January 31, 2025
Accepted: February 21, 2025

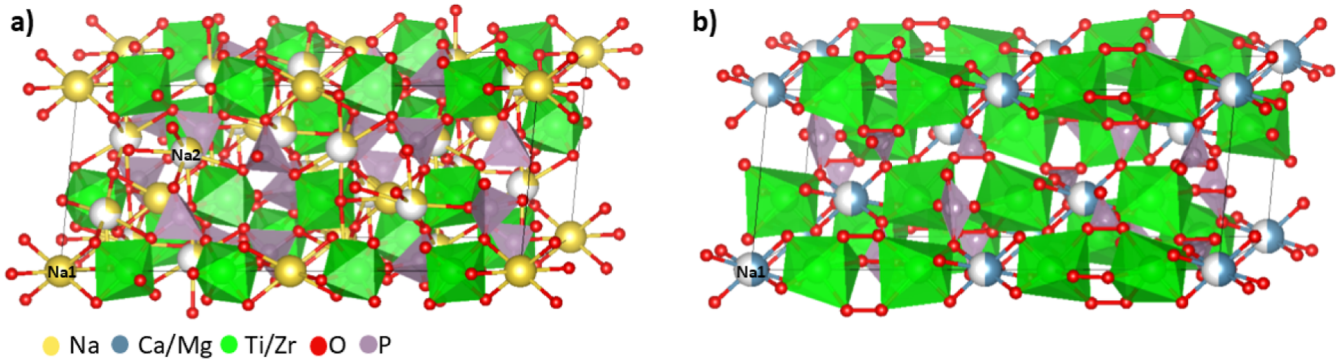

Figure 1. (a) Rhombohedral unit cell of the classical NASICON phase. Na1 sites are fully occupied, and Na2 sites are occupied partially. (b) Rhombohedral unit cell of the NASICON phase with Mg or Ca instead of Na. Na1 sites are half occupied, and Na2 sites are not occupied in the ground state.

In times of energy crisis and more demand for electrical storage both in homes and vehicles, the design of new battery systems which do not rely on lithium and, more importantly, on the fast depleting cobalt is in high demand.[6] An obvious choice for higher capacity, especially when the size of the battery is important, is multivalent charge carriers. A promising candidate here is calcium[12,13] as it additionally does not form dendrites and is very abundant in the Earth's crust. Furthermore, all-solid batteries have drawn a lot of attention in recent times,[14] and the NASICON structure is a popular choice as a solid electrolyte, which has been tested intensively with different transition metals and dopants. Also, sodium as a charge carrier has been partially or fully replaced with lithium or multivalent magnesium.[13,15−17] It can also be utilized as an electrode material under the constraint of electronic conductibility.[11] However, batteries based on multivalent charge carriers are plagued by a lower ion mobility in solid battery materials due to their larger electrostatic interaction with the host lattice.[18,19]

This work explores potential differences in ion mobility within NASICON phases, where sodium is fully substituted by calcium. NASICON materials offer a wide range of transition metal options, and we focus on comparing the zirconium-based phase with the titanium-based phase because of their shared group in the periodic table, meaning they contribute the same number of electrons to redox reactions. However, their different atomic sizes may influence ion mobility, particularly with respect to the so-called bottleneck size, which determines the minimum energy barrier for diffusion. This work aims to investigate how these size differences impact the overall ion mobility within the system.

COMPUTATIONAL DETAILS

All phases were studied using periodic density functional theory,[20,21] as implemented in the Vienna Ab initio Simulation Package,[22,23] which has been shown to be well-suited to model the properties of batteries.[24] The electron−core interactions are represented by the Projector Augmented Wave[25] method. Calculations were first performed for the rhombohedral unit cells of the two NASICON phases consisting of 6 formula units each with the Brillouin zone sampled using a $4 \times 4 \times 1$ k-point grid. For adsorption, intercalation, and ion diffusion, different supercells, which are specified in the respective sections, were used, and the k-point grid was scaled accordingly in each lattice direction.

The electronic structure was converged to 1×10^{-5} eV, applying a plane-wave cutoff energy of 550 eV. The calculations have been performed without taking spin-polarization into account, as only the nonmagnetic metals Ti and Zr were considered and previous calculations[16] did not find any significant spin-polarization in Ti-containing NASICON materials. The migration barriers for intercalation and bulk diffusion were obtained by applying the climbing image Nudged Elastic Band (NEB) method.[26] Most NEB calculations were performed by using three distinct images along the pathway. The ones which required more detailed calculations were found in preliminary setups to be symmetrical with a metastable state in the middle and were thus calculated in a symmetrical fashion from the start point to the metastable intermediate state. All forces on the atoms were converged within 0.05 eV $Å^{-1}$. All cells were calculated in a charge-neutral fashion, which is the stable state for macroscopic solid materials.[10]

RESULTS AND DISCUSSION

Ordering. In this paper, we consider Ca insertion in the classical NASICON structures of $Ca_yM_2(PO_4)_3$ with M = Ti and Zr adapted from experimental X-ray diffraction (XRD) data.[27] As already mentioned above, they have been chosen because they have the same number of valence electrons but differ in size, with the Zr ion being about 15% larger than the Ti ion. The considered phases show a rhombohedral structure. As the acronym NASICON, sodium (Na) superionic conductor, already suggests, these materials have originally been used as solid electrolytes for sodium ion batteries.[28] However, they have recently also become of interest as possible electrode materials for calcium-ion batteries.[11] Given the oxidation states of the considered elements, the Ca-NASICON structures will, in general, be able to remain electrostatically neutral for an occupation of $0.5 \leq y \leq 2.5$ calcium per formula unit.

The rhombohedral unit cell of the NASICON structure contains six formula units (Figure 1). With the monovalent sodium NASICON structure, at least one Na atom per formula unit is needed to form a charge-neutral cell. However, for the divalent Ca and Mg cations, only half a cation per formula unit (or one cation per two formula units) is needed. It is still typical to refer to the Ca stoichiometry as one formula unit as in $Ca_yM_2(PO_4)_3$,[11] which then results in a nomenclature in which a site occupancy of 0.5 is assumed. This nomenclature is also motivated by the results of XRD experiments, which yield

https://doi.org/10.1021/acs.jpcc.4c08058
J. Phys. Chem. C XXXX, XXX, XXX−XXX

that the Ca atom can sit at equivalent Na1 sites of the sodium atom in the standard NASICON phase, yielding a likelihood of 0.5 for occupation of one particular site.[27] These Na1 sites in a traditional NASICON phase (6B Wyckoff site) sit in an elongated octahedra, while the so-called Na2 sites are left empty and only passed during diffusion from one Na1 site to the next in the studied systems.

In our calculations, the previously described rhombohedral NASICON structure ($R\bar{3}c$) ($Ca_xM_{12}(PO_4)_{18}$) containing six NASICON formula units was utilized for all calculations. We also use this stoichiometry to denote the Ca concentrations x considered in this computational study, as it avoids ambiguity associated with the 0.5 occupancies when discussing the differently occupied systems at the high vacancy limit. In the y = 0.5 occupancy, three cations are to be distributed among six distinct sites, which are all equal in energy for a single occupancy within the rhombohedral unit cell, yielding 20 possible distinct occupation patterns inside the unit cell. However, the variation in the mutual distances between the three cations depending on the particular distribution leads to a variation in the interaction strength, causing an energetic ordering of these symmetrically inequivalent occupation patterns. Our calculations showed that the occupation patterns, where alternating sites along the z axis are occupied, are the most stable. This is most likely due to their maximum distance between the cations. They are closely followed in stability by the systems in which two neighboring sites are occupied, and the most unstable variations are present when the cations sit right next to each other. However, these stabilities vary by less than 5 meV per atom and suggest that the preference for the cations to be spread equally inside the unit cell with no clustering is present but small (see Table 1).

Table 1. Differences Between the Orderings in meV Per Atom in the $Ca_3M_{12}(PO_4)_{18}$ Unit Cells

	M = Ti	M = Zr
first step	4.1	3.6
second step	2.0	6.5

In order to verify the most stable configurations, we employed a larger 2 × 2 × 1 supercell for the NASICON structure. Initially, various occupation scenarios were randomly selected as well as options with the highest symmetry. Those were cells with altering layers fully filled, as well as neighboring layers fully filled. In total, 95 potential occupation arrangements were investigated. Within this context, the cations exhibited a preference for repeatedly occupying the same site within neighboring unit cells, which led to the formation of distinct layers. Among these configurations, the most stable arrangement involved three layers that were fully occupied, while their alternating three layers remained entirely empty. However, the total difference between the highest and lowest energy per atom in the system varied by less than 10 meV, indicating the weak mutual interaction between the Ca atoms. The open-circuit voltage with respect to a Ca metal anode for an occupation from 0 to 6 Ca per rhombohedral unit cell was checked for possible use as an electrode material. These numbers are determined by calculating the energy gain upon transferring one Ca atom from a Ca metal to NASICON materials. As Ca acts as a bivalent ion, the corresponding energy gain in eV has to be divided by two in order to get the open circuit voltage.[29] Note that in batteries, only materials with an insertion energy that is positive with respect to the metal cohesion energy can be used because otherwise the metal atoms would not penetrate the material but exhibit plating. Large open circuit voltages suggest the use of the corresponding material as the cathode and low open circuit voltages as anode materials. The trends are the same for both phases, and the exact voltages are shown in Table 2: The first

Table 2. Insertion Voltages in V for x Ca Atoms into the $Ca_xM_{12}(PO_4)_{18}$ Phase With M = Ti and Zr

x	1	2	3	4	5	6
Ti	16.4	4.7	4.8	−0.9	1.6	1.3
Zr	7.9	4.6	4.7	−3.0	0.5	0.2

intercalation voltage is very high, with 16.4 V for the Ti phase and 7.9 V for the Zr phase. Note that these high voltages are simply due to the fact that the NASICON material is extremely unstable in the absence of any inserted ion, so the numbers are of no practical relevance. The second and third insertion voltages are both about 4.7 V for both phases. The fourth Ca has a negative voltage and, thus, is not a stable phase. The stability of the structure for x = 3 can be simply explained based on stoichiometry arguments. At x = 3, the oxidation numbers of Ca (2+), Ti or Zr (4+), and PO_4 (3−) match to yield a total oxidation number of 0. The addition of one more Ca atom then leads to a nonstoichiometric structure that is unstable. It is also important to note that for the fourth Ca atom, the Na2 positions become more stable for further occupation than the Na1 positions. Going from the fourth to the fifth Ca, the voltage is positive for both phases again, making this transition from four cations to five possible. The occupation with six Ca is most stable with three Ca in the Na1 positions and three in the Na2 positions. These voltages show nicely that the material might only be suitable as a cathode material in the 1−3 occupation window but is generally more suitable as a solid electrolyte.

Diffusion. In a typical NASICON material, the Na cations diffuse through the Na1−Na2−Na1 pathway. In the Ca case, the only difference is that the Na2 equivalent position is much less stable compared to the Na1 position, transforming it into a metastable intermediate state instead of a partially occupied site. Therefore, a full diffusion event takes place between two neighboring Na1 positions. Along the minimum energy path for diffusion, the migrating ion has to pass through a triangular area consisting of the three oxygen atoms in the PO_4 tetrahedron and the TiO_6 or ZrO_6 octahedron, respectively. It has been suggested to consider the area of this bottleneck that corresponds to the structure with the smallest opening along the diffusion pathway as a descriptor for the activation energy for diffusion.[13,30,31] Note that at the same time, this bottleneck structure corresponds to the location of the minimum energy barrier for diffusion. As shown in Figure 2, there are two such bottlenecks denoted by A1 and A2 in the pathway from Na1 to the Na2 intermediate site, which corresponds to a local minimum along the diffusion path. The octahedron at the Na2 site is slightly smaller than the one at the Na1 site, so the area of its triangular faces, marked as A2 in the figure, corresponds to the defining bottleneck. It has an area of 4.67 $Å^2$ for the Ti phase and 5.98 $Å^2$ for the Zr phase. The bottleneck in the Ti phase is thus significantly smaller and only 80% of the area in the Zr phase, suggesting that diffusion

https://doi.org/10.1021/acs.jpcc.4c08058
J. Phys. Chem. C XXXX, XXX, XXX−XXX

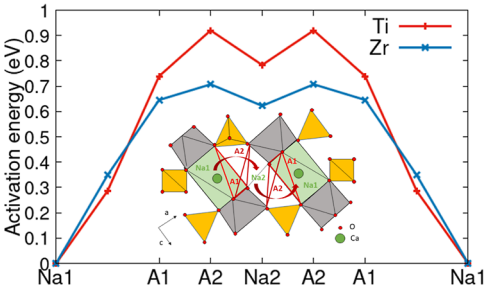

Figure 2. NEB pathway of the diffusion event for one Ca moving through the two bottlenecks and the metastable intermediate in the different phases with a representation of the diffusion pathway of Ca through the NASICON structures. Ca moves through the first octahedra plane A1, then A2 into the unoccupied metastable Na2 site, then again through A2 and A1 into the next Na1 site. The bottleneck of the diffusion is A2 because of its slightly smaller size. The yellow tetrahedra and gray octahedra correspond to PO_4 and the TiO_6 or ZrO_6 units, respectively.

will be more hindered in the Ti phase, i.e., associated with a higher diffusion barrier than the Zr phase.

Now we discuss the energy barriers for migration derived from NEB calculations. As a first step, we check the diffusion energy of only one cation to exclude all influence of different occupational environments on the diffusion pathway. This calculation yielded, for the $Ca_1Ti_{12}(PO_4)_{18}$, a barrier of 0.92 eV and, for $Ca_1Zr_{12}(PO_4)_{18}$, a barrier of 0.71 eV. For both isostructural cells, the energy barriers were roughly the same between all six possible sites with a variance of 5 meV, showing them to be of the same symmetry. Also, the prediction of the bottleneck size holds true, as the Zr barrier is only 77% as high as the Ti barrier. Figure 2 shows that the diffusion pathway for one isolated Ca atom is symmetric with respect to the metastable Na2 site. This symmetry can become broken for higher Ca occupations in the simulation cell. For symmetric environments, only half of the total pathway was calculated and then mirrored to the other half to save calculation time. This is the case for most pathways with an occupation of three cations and for all pathways with only one cation present. The following systems with an asymmetrical environment of cations were determined in two sections with the intermediate positions as a start and end point for ease of calculation.

Adding another cation into the cells creates three distinct pathways of diffusion for each occupational site in the system because of symmetry: The first where the diffusing atom diffuses away from the other cation, the second where it diffuses toward, and then the third where the diffusing cation moves parallel to the other cation, which lies in the other half of the unit cell along the z axis, and thus has maximum distance to the diffusion pathway. These three environments are present for all six pathways in the large rhombohedral unit cell. We performed the calculations for the three environments using only one of the six pathways because the calculations with one cation showed those six to be energetically equivalent. As described before, they are asymmetrical pathways in which the higher barrier is the determining step. Both isostructural cells (with Ti or Zr) showed the same trend: The closer the

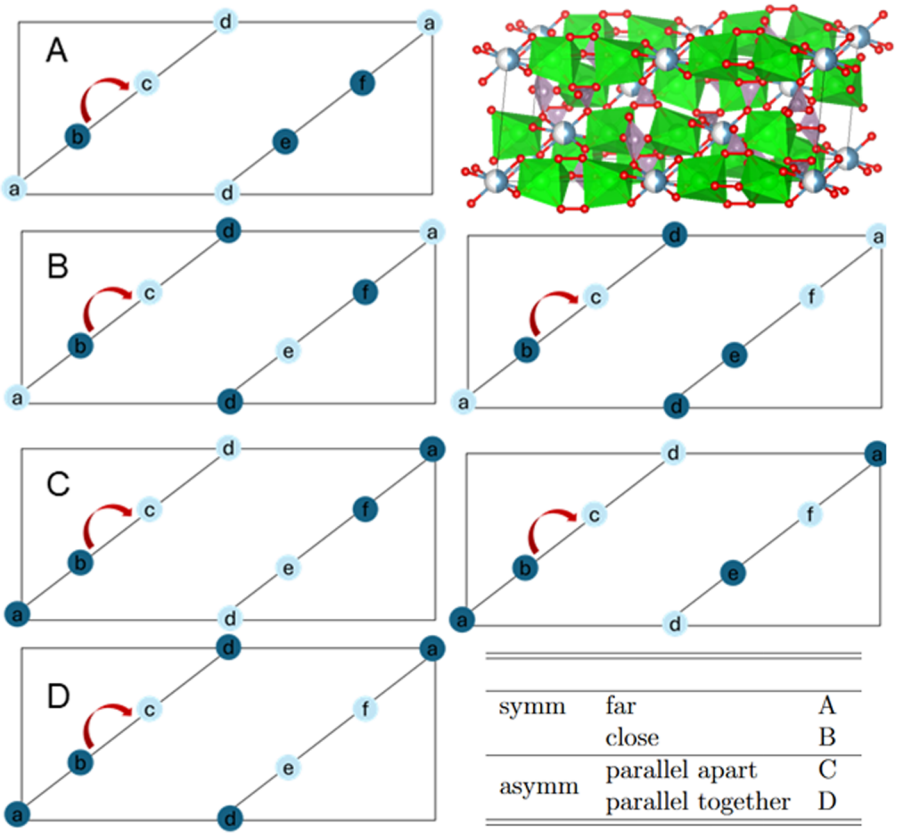

symm	far	A
	close	B
asymm	parallel apart	C
	parallel together	D

Figure 3. Simplified schematic rhombohedral unit cell showing the four distinct pathway symmetries possible for each diffusion from Na1 to another Na1 site on the example of one specific diffusion event. Bold positions are occupied, and faint ones are unoccupied. The arrow marks the diffusion.

https://doi.org/10.1021/acs.jpcc.4c08058
J. Phys. Chem. C XXXX, XXX, XXX−XXX

additional cation is to the diffusion process, the higher the barrier gets. For the Ti phase, the barriers where the cation diffuses toward and away from the additional cation both lie at 1.01 eV, and when the cation is further away on the parallel, the barrier is 0.89 eV. For the Zr phase, the farther barriers are 0.76 eV, and the closer one is 0.61 eV.

With all three cations present, there are four distinct pathways, which can be seen in Figure 3. Two of them are symmetric with the two other cations either being on either side of the diffusion process (B), which is very close to the diffusion pathway, and in the second case parallel to it (A), which is the furthest the cations can be away from the diffusion. The other two are asymmetric with the cations either directly next to each other (D) or spread out in the phase (C).

In the resulting barrier heights from these possible environments shown in Table 3, it can again be confirmed that in the studied systems, the closer the other cations are to the diffusing cation, the higher the barrier is. It has already been previously suggested that the Coulomb repulsion between two neighboring metal cations leads to an increase in the barrier heights.[32] Hence, one would naively think that larger Ca concentrations should lead to higher diffusion barriers. However, as Table 4 shows, with additional Ca atoms present in the cell further from the diffusion event, the barriers are lower than for the single atom diffusion. Thus, obviously a balanced distribution of the Ca atoms in the unit cell reduces the effective Coulomb repulsion close to the transition state, as illustrated in Figure 3. In Figure 4 and Table 4, a direct comparison is shown between the minimum diffusion barrier for both materials. It can here be seen that the diffusion barrier in the Zr phase is consistently lower than in the Ti phase. Note that typically 650 meV are assumed as the maximum diffusion barrier that would still allow sufficient charge/discharge rates in solid materials.[33,34] Hence, $Ca_xTi_{12}(PO_4)_{18}$ with $x = 3$ and $Ca_xZr_{12}(PO_4)_{18}$ with $x = 2$ and 3 can be considered as suitable solid electrolyte materials.

Table 3. Diffusion Barrier in eV for the Two Isostructural Systems $Ca_3M_{12}(PO_4)_{18}$ for One Ca With Two Other Ca Atoms Present in the System

			M = Ti	M = Zr
symm	far	A	0.64	0.41
	close	B	1.22	0.92
asymm	parallel apart	C	0.98	0.67
	parallel together	D	1.01	0.85

Table 4. Minimum Diffusion Barrier in eV for the Two Considered NASICON Materials With Three Different Ca Concentrations

	$x = 1$	$x = 2$	$x = 3$
$Ca_xTi_{12}(PO_4)_{18}$	0.92	0.89	0.64
$Ca_xZr_{12}(PO_4)_{18}$	0.71	0.61	0.41

It is also important to emphasize that there is a substantial reduction in the diffusion barriers for higher Ca concentrations. Similar computational results have also been found upon the co-intercalation of Na into $Ca_xNa_yV_2(PO_4)_3$ phases[32] and are congruent with the results of the insertion voltages. A study of the NASICON-type material as a cathode material for Ca batteries showed similar behavior for $Ca_xV_2(PO_4)_3$, but the opposite behavior has been observed for $Ca_xMn_2(PO_4)_3$.[11] This is a hint that the studied materials are indeed more suited as a solid electrolyte rather than an electrode material.

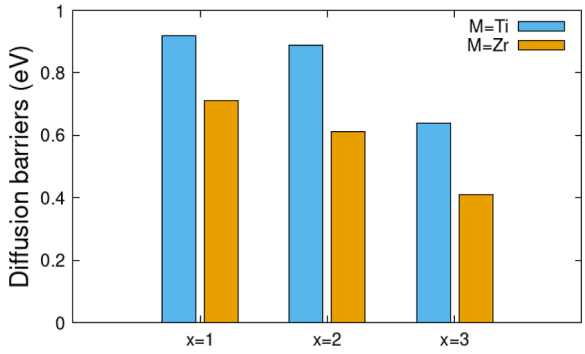

Figure 4. Minimum diffusion barrier in eV for the two considered NASICON materials, $Ca_xM_{12}(PO_4)_{18}$ with three different Ca concentrations, $x = 1$, 2, and 3 (M = Ti/Zr).

CONCLUSIONS AND SUMMARY

In this computational study, we have addressed the Ca mobility in NASICON battery materials from first principles. Due to the complex structure of the NASICON material, the determination of the Ca migration paths is computationally rather demanding, limiting the number of systems that can be numerically studied. In particular, we considered Ca mobility in Ti- and Zr-based NASICON materials. These two metals have the same number of valence electrons but different sizes; the Zr ion is about 14% larger than the Ti ion, which makes the crystal structure more open. According to our calculations, both materials can act as suitable solid electrolytes in Ca-ion batteries. The triangular faces of the so-called Na2 octahedra correspond to the bottleneck along the diffusion path, with the area of the faces of the TiO_6 octahedron being 20% smaller than those of the ZrO_6 octahedron. In fact, we find that the Zr barrier for Ca diffusion is 23% smaller than the Ti barrier, confirming the notion that the size of the bottlenecks acts as a good descriptor for the ion mobility. This suggests that increasing the size of the bottlenecks, for example, by deliberately doping the NASICON material with larger metal ions, provides a route for increasing the ion mobility in these structures.

ASSOCIATED CONTENT

Data Availability Statement

The data that support the findings of this study are openly available under the Creative Commons Attribution license (CC BY 4.0) on the NOMAD repository (https://nomad-lab.eu) within the data set "Ca mobility in NASICON battery materials studied from first-principles", DOI: 10.17172/NOMAD/2025.01.31-1.

AUTHOR INFORMATION

Corresponding Author

Katharina Helmbrecht − *Institute of Theoretical Chemistry, Ulm University, 89081 Ulm, Germany*; Email: katharina.helmbrecht@uni-ulm.de

Author

Axel Groß − *Institute of Theoretical Chemistry, Ulm University, 89081 Ulm, Germany; Helmholtz Institute Ulm*

https://doi.org/10.1021/acs.jpcc.4c08058
J. Phys. Chem. C XXXX, XXX, XXX−XXX

(HIU) for Electrochemical Energy Storage, 89081 Ulm, Germany; orcid.org/0000-0003-4037-7331

Complete contact information is available at: https://pubs.acs.org/10.1021/acs.jpcc.4c08058

Notes

The authors declare no competing financial interest.

■ ACKNOWLEDGMENTS

This work contributes to the research performed at CELEST (Center for Electrochemical Energy Storage Ulm-Karlsruhe) and was funded by the Deutsche Forschungsgemeinschaft (DFG, German Research Foundation) under Germany's Excellence Strategy—EXC 2154—Project number 390874152 (POLiS Cluster of Excellence). The computer time was provided by the state of Baden-Württemberg through bwHPC and the German Research Foundation (DFG) through grant no INST 40/575-1 FUGG (JUSTUS 2 cluster).

■ REFERENCES

(1) Goodenough, J. B.; Park, K.-S. The Li-Ion Rechargeable Battery: A Perspective. *J. Am. Chem. Soc.* **2013**, *135*, 1167−1176.
(2) Larcher, D.; Tarascon, J.-M. Towards greener and more sustainable batteries for electrical energy storage. *Nat. Chem.* **2015**, *7*, 19−29.
(3) Vaalma, C.; Buchholz, D.; Weil, M.; Passerini, S. A cost and resource analysis of sodium-ion batteries. *Nat. Rev. Mater.* **2018**, *3*, 18013.
(4) Vinayan, B. P.; Euchner, H.; Zhao-Karger, Z.; Cambaz, M. A.; Li, Z.; Diemant, T.; Behm, R. J.; Groß, A.; Fichtner, M. Insights into the electrochemical processes of rechargeable magnesium−sulfur batteries with a new cathode design. *J. Mater. Chem. A* **2019**, *7*, 25490−25502.
(5) Maroni, F.; Dongmo, S.; Gauckler, C.; Marinaro, M.; Wohlfahrt-Mehrens, M. Through the Maze of Multivalent-Ion Batteries: A Critical Review on the Status of the Research on Cathode Materials for Mg^{2+} and Ca^{2+} Ions Insertion. *Batteries Supercaps* **2021**, *4*, 1221−1251.
(6) Esser, B.; Ehrenberg, H.; Fichtner, M.; Groß, A.; Janek, J. Post-Lithium Storage—Shaping the Future. *Adv. Energy Mater.* **2025**, *15*, 2402824.
(7) Wang, Y.; Song, S.; Xu, C.; Hu, N.; Molenda, J.; Lu, L. Development of solid-state electrolytes for sodium-ion battery − A short review. *Nano Mater. Sci.* **2019**, *1*, 91−100.
(8) Alamo, J. Chemistry and properties of solids with the [NZP] skeleton. *Solid State Ionics* **1993**, *63*, 547−561.
(9) Entwistle, J.; Zhang, L.; Zhang, H.; Tapia-Ruiz, N. In *Comprehensive Inorganic Chemistry III*, 3rd ed.; Reedijk, J., Poeppelmeier, K. R., Eds.; Elsevier: Oxford, 2023; pp 199−215.
(10) Sotoudeh, M.; Baumgart, S.; Dillenz, M.; Döhn, J.; Forster-Tonigold, K.; Helmbrecht, K.; Stottmeister, D.; Groß, A. Ion Mobility in Crystalline Battery Materials. *Adv. Energy Mater.* **2024**, *14*, 2302550.
(11) Tekliye, D. B.; Kumar, A.; Weihang, X.; Mercy, T. D.; Canepa, P.; Sai Gautam, G. Exploration of NaSICON Frameworks as Calcium-Ion Battery Electrodes. *Chem. Mater.* **2022**, *34*, 10133−10143.
(12) Bier, D.; Li, Z.; Klyatskaya, S.; Sbei, N.; Roy, A.; Riedel, S.; Fichtner, M.; Ruben, M.; Zhao-Karger, Z. Long Cycle-Life Ca Batteries with Poly(anthraquinonylsulfide) Cathodes and Ca-Sn Alloy Anodes. *ChemSusChem* **2023**, *16*, No. e202300932.
(13) Wei, Z.; Singh, D. K.; Helmbrecht, K.; Sann, J.; Yusim, Y.; Kieser, J. A.; Glaser, C.; Rohnke, M.; Groß, A.; Janek, J. In Situ Observation of Room-Temperature Magnesium Metal Deposition on a NASICON/IL Hybrid Solid Electrolyte. *Adv. Energy Mater.* **2023**, *13*, 2302525.
(14) Janek, J.; Zeier, W. G. A solid future for battery development. *Nat. Energy* **2016**, *1*, 16141.
(15) Jian, Z.; Hu, Y.-S.; Ji, X.; Chen, W. NASICON-Structured Materials for Energy Storage. *Adv. Mater.* **2017**, *29*, 1601925.
(16) Fami, A.; Wahab, N.; Rani, M.; Yaakob, M.; Mustaffa, N. First Principles Investigation of NASICON-Structured $LiTi_2(PO_4)_3$ and $Mg_{0.5}Ti_2(PO_4)_3$ Solid Electrolytes. *Int. J. Electrochem. Sci.* **2022**, *17*, 220115.
(17) Rutt, A.; Shen, J.-X.; Horton, M.; Kim, J.; Lin, J.; Persson, K. A. Expanding the Material Search Space for Multivalent Cathodes. *ACS Appl. Mater. Interfaces* **2022**, *14*, 44367−44376.
(18) Bachman, J. C.; Muy, S.; Grimaud, A.; Chang, H.-H.; Pour, N.; Lux, S. F.; Paschos, O.; Maglia, F.; Lupart, S.; Lamp, P.; et al. Inorganic Solid-State Electrolytes for Lithium Batteries: Mechanisms and Properties Governing Ion Conduction. *Chem. Rev.* **2016**, *116*, 140−162.
(19) Sotoudeh, M.; Groß, A. Descriptor and Scaling Relations for Ion Mobility in Crystalline Solids. *JACS Au* **2022**, *2*, 463−471.
(20) Hohenberg, P.; Kohn, W. Inhomogeneous Electron Gas. *Phys. Rev.* **1964**, *136*, B864−B871.
(21) Kohn, W.; Sham, L. J. Self-Consistent Equations Including Exchange and Correlation Effects. *Phys. Rev.* **1965**, *140*, A1133−A1138.
(22) Kresse, G.; Furthmüller, J. Efficient iterative schemes for ab initio total-energy calculations using a plane-wave basis set. *Phys. Rev. B* **1996**, *54*, 11169−11186.
(23) Kresse, G.; Joubert, D. From ultrasoft pseudopotentials to the projector augmented-wave method. *Phys. Rev. B* **1999**, *59*, 1758−1775.
(24) Euchner, H.; Groß, A. Atomistic modeling of Li- and post-Li-ion batteries. *Phys. Rev. Mater.* **2022**, *6*, 040302.
(25) Blöchl, P. E. Projector augmented-wave method. *Phys. Rev. B* **1994**, *50*, 17953−17979.
(26) Sheppard, D.; Terrell, R.; Henkelman, G. Optimization methods for finding minimum energy paths. *J. Chem. Phys.* **2008**, *128*, 134106.
(27) Rashmi, C.; Shrivastava, O. Synthesis and crystal structure of nanocrystalline phase: $Ca_{1-x}M_xZr_4P_6O_{24}$ (M = Sr, Ba and x = 0.0−1.0). *Solid State Sci.* **2011**, *13*, 444−454.
(28) Singh, B.; Wang, Z.; Park, S.; Gautam, G. S.; Chotard, J.-N.; Croguennec, L.; Carlier, D.; Cheetham, A. K.; Masquelier, C.; Canepa, P. A chemical map of NaSICON electrode materials for sodium-ion batteries. *J. Mater. Chem. A* **2021**, *9*, 281−292.
(29) Islam, M. S.; Fisher, C. A. J. Lithium and sodium battery cathode materials: computational insights into voltage, diffusion and nanostructural properties. *Chem. Soc. Rev.* **2014**, *43*, 185−204.
(30) Martinez-Juarez, A.; Pecharromán, C.; Iglesias, J. E.; Rojo, J. M. Relationship between Activation Energy and Bottleneck Size for Li^+ Ion Conduction in NASICON Materials of Composition $LiMM'(PO_4)_3$;M, M' = Ge, Ti, Sn, Hf. *J. Phys. Chem. B* **1998**, *102*, 372−375.
(31) Wang, Q.; Gao, H.; Li, J.; Liu, G.-B.; Jin, H. Importance of Crystallographic Sites on Sodium-Ion Extraction from NASICON-Structured Cathodes for Sodium-Ion Batteries. *ACS Appl. Mater. Interfaces* **2021**, *13*, 14312−14320.
(32) Blanc, L. E.; Choi, Y.; Shyamsunder, A.; Key, B.; Lapidus, S. H.; Li, C.; Yin, L.; Li, X.; Gwalani, B.; Xiao, Y.; et al. Phase Stability and Kinetics of Topotactic Dual Ca^{2+}-Na^+ Ion Electrochemistry in NaSICON $NaV_2(PO_4)_3$. *Chem. Mater.* **2023**, *35*, 468−481.
(33) Canepa, P.; Sai Gautam, G.; Hannah, D. C.; Malik, R.; Liu, M.; Gallagher, K. G.; Persson, K. A.; Ceder, G. Odyssey of Multivalent Cathode Materials: Open Questions and Future Challenges. *Chem. Rev.* **2017**, *117*, 4287−4341.
(34) Döhn, J.; Groß, A. Computational Screening of Oxide Perovskites as Insertion-Type Cathode Material. *Adv. Energy Sustainability Res.* **2024**, *5*, 2300204.